# Spatially Distributed Measurements of Platform Motion for the Correction of Ship-Based Turbulent Fluxes

IAN M. BROOKS

*School of Earth and Environment, University of Leeds, Leeds, United Kingdom*

(Manuscript received 29 October 2007, in final form 14 March 2008)

ABSTRACT

A method for determining the angular offsets between measurement axes for multiple motion sensing systems and a sonic anemometer using underway data is demonstrated. This enables a single angular rate sensor to be used with spatially separated accelerometers, collocated with sonic anemometers, for the motion correction of turbulence measurements on a mobile platform such as a ship. Effective motion correction of turbulence measurements at sea is demonstrated. The errors in instrument alignment are considered, and estimates are made of the resulting biases in wind stress estimates.

## 1. Introduction

Eddy covariance is the most direct technique for the estimation of turbulent fluxes. Its application on mobile platforms such as ships, buoys, or aircraft requires the correction of the components of the wind velocity vector, measured in a reference frame fixed with respect to the platform, for the changing attitude and velocity of the platform. The basic theory behind such corrections is well documented (Lenschow 1986; Lenschow and Spyers-Duran 1989; Anctil et al. 1994; Edson et al. 1998; Schulze et al. 2005), but requires care in its application due to differences between systems, both in the basic measured quantities and in sign conventions and the choice of coordinate systems. For ship- and buoy-based installations, a common choice of measurement system has been a combination of high-frequency measurements from collocated three-axis linear accelerometers and angular rate gyros, coupled with a low-frequency measurement of the magnetic compass heading (Edson et al. 1998; Anctil et al. 1994; Graber et al. 2000). Edson et al. (1998) discuss in detail the use of such a system to determine platform motion and attitude. It is desirable to locate the motion pack close to the wind measurement volume—here the sensing head of a sonic anemometer—in order to minimize the vector offset between the points of measurement of the wind and acceleration vectors, and hence the magnitude of the linear velocity imposed at the point of wind measurement by its rotation around the accelerometers.

During a research cruise on the RRS *Discovery* (cruise D317) for the Sea Spray, Gas Flux and Whitecap Experiment (SEASAW; Brooks et al. 2007), a contribution to the U.K. Surface-Ocean/Lower Atmosphere Study (U.K.-SOLAS), two independent turbulence systems were installed on the foremast (Fig. 1). The first system, installed by the National Oceanography Centre, Southampton (NOCS), consisted of Gill R3 sonic anemometers located at the forward corners on either side of the foremast platform. A Systron Donner MotionPak was located just aft of the base of the starboard anemometer. The accelerations and rotation rates were sampled synchronously with the wind components via the anemometer's analog input channels. The second system was installed by the University of Leeds at the top of the foremast, and consisted of a Gill R3 sonic anemometer with a motion pack designed and built at Leeds consisting of a three-axis linear accelerometer and a commercial pitch, roll, and magnetic compass heading sensor, both rigidly mounted on a control and communications board and logged via an RS485 serial line. Both installations were sampled at 20 Hz. Failure of the pitch/roll/heading sensor in the Leeds system forced us to utilize the rotation rate measurements from the Systron Donner MotionPak. This paper discusses the combination of data from spatially sepa-

*Corresponding author address:* Dr. Ian M. Brooks, Institute for Atmospheric Science, School of Earth and Environment, University of Leeds, Leeds LS2 9JT, United Kingdom.
E-mail: i.brooks@see.leeds.ac.uk

DOI: 10.1175/2008JTECHA1086.1

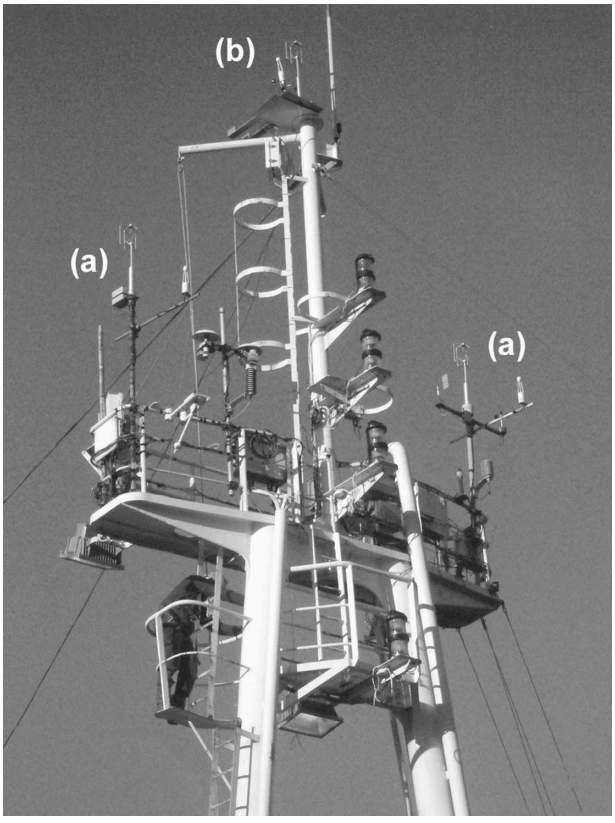


FIG. 1. Foremast of the RRS *Discovery* showing the turbulence instrumentation from (a) NOCS and (b) Leeds.

rated motion systems. While the necessity of such an approach was forced upon us, the techniques used here are more widely applicable and provide a means for effectively combining data from a single highly specified motion pack with that from cheap spatially distributed accelerometers, collocated with sonic anemometers, for the correction of turbulence measurements without the need to determine the precise vector offsets between the widely separated systems.

## 2. Methodology

Rotation rates and attitude angles measured at a single point are valid everywhere on the platform, while linear accelerations vary considerably with distance from the center of rotation. We can thus utilize a single integrated motion pack incorporating both accelerometers and angular rate sensors, along with simple linear accelerometers at separate locations to enable motion correction of turbulent wind measurements without having to determine the large vector offsets between installation sites, provided that the angular offsets between measurement axes are known or can be determined. A method for determining the angular offsets between the systems from in situ, underway data records is presented below, and the correction of turbulent wind measurements at an anemometer remote from the integrated motion pack is demonstrated.

On the RRS *Discovery* both turbulence systems were oriented toward the bow; however, no attempt was made to align them precisely with each other. The principal measurement axes are chosen to be a right-handed Cartesian system with $x$ positive toward the bow, $y$ positive to port, and $z$ positive upward. Rotations are defined as a set of three Euler angles, that is, rotations about nonorthogonal axes where each rotation is about one of the axes resulting from the previous rotation: yaw ($\gamma$), positive for a right-handed rotation about the $z$ axis; pitch ($\alpha$), positive for an upward tilt of the $x$ axis (note this is a left-handed rotation); and roll ($\beta$), positive for an upward tilt of the $y$ axis. The orientation of the measurement frame with respect to the required reference frame is obtained by applying the rotations in order: yaw, pitch, roll. To transform the measurements back to the desired reference frame, the opposite rotations are applied in reverse order; in vector notation this is

$$\mathbf{V} = \mathbf{YPRV}', \tag{1}$$

where $\mathbf{V}$ is a vector quantity and the prime indicates the measurement frame. In addition, $\mathbf{Y}$, $\mathbf{P}$, and $\mathbf{R}$ are the yaw, pitch, and roll rotation matrices, respectively:

$$\mathbf{Y} = \begin{bmatrix} \cos\gamma & -\sin\gamma & 0 \\ \sin\gamma & \cos\gamma & 0 \\ 0 & 0 & 1 \end{bmatrix},$$

$$\mathbf{P} = \begin{bmatrix} \cos\alpha & 0 & -\sin\alpha \\ 0 & 1 & 0 \\ \sin\alpha & 0 & \cos\alpha \end{bmatrix},$$

$$\mathbf{R} = \begin{bmatrix} 1 & 0 & 0 \\ 0 & \cos\beta & -\sin\beta \\ 0 & \sin\beta & \cos\beta \end{bmatrix}. \tag{2}$$

Once the pitch and roll offsets of each system from a common $x$–$y$ plane, and the yaw offset between them in that plane, are determined, we can transform the measurements from one system ($a$) to the reference frame of the other ($b$) by

$$\mathbf{V}_b = \mathbf{R}_b'\mathbf{P}_b'\mathbf{YP}_a\mathbf{R}_a\mathbf{V}_a, \tag{3}$$

where subscripts indicate system $a$ or $b$ and primes indicate inverse matrices. To determine the attitude and motion corrections required for the Leeds sonic anemometer, we combine the accelerations from the Leeds system with the rotation rates from the NOCS motion pack, rotated into the Leeds system reference frame via (3).

### a. Synchronization of time series

The two systems used during SEASAW were logged independently and suffered a small time offset between the two datastreams that varied between about 1 and 3 s from record to record, and resulting from the delay in initializing the serial interfaces on the NOCS system at the start of each data file (note, however, that all datastreams on either system are internally synchronized). This offset was determined via a correlation analysis of the vertical accelerations from the two systems for each contiguous data record. Figure 2 shows the vertical accelerations from the two systems for a 25-s period of the data record, before and after correction of the time lag.

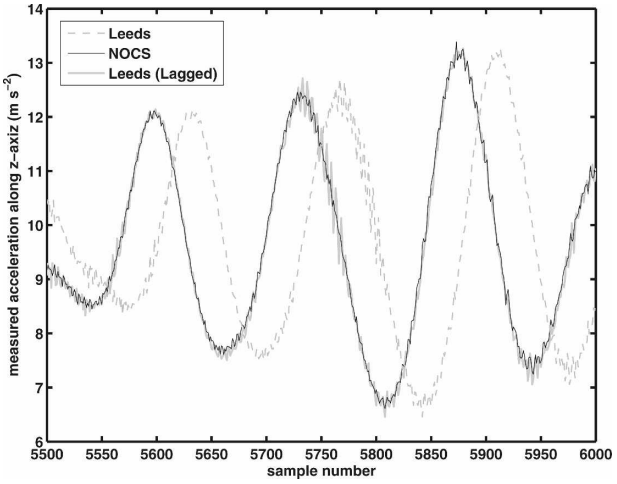


FIG. 2. A 25-s section of the raw measured accelerations along the $z$ axes of the Leeds and NOCS systems before and after correction of the time lag between them.

### b. Alignment of reference frames

The first step in determining the angular offsets between the two systems is to calculate their respective mean pitch and roll angles from the true horizontal plane. This is achieved by low-pass filtering the accelerations along the $x$ and $y$ axes to remove the motion-induced variations. The tilts of the $x$ and $y$ axes from the horizontal are given by $\sin^{-1}(a/g)$, where $a$ is the mean low-pass-filtered acceleration along the axis in question over a period of at least several times the filter period, and $g$ is gravity. Here, we choose a filter passband period of 4 min and a cutoff period of 2 min—much longer than the observed wave periods of between approximately 8 and 25 s. Filtering is performed in the frequency domain by taking the Fourier transform of the time series, setting the Fourier coefficients in the stop band to zero, and applying a cosine rolloff between the passband corner and cutoff frequencies; the inverse Fourier transform is then applied to recover the filtered time series. This approach avoids distortions at the ends of the time series that can affect digital filters applied in the time domain (e.g., Edson et al. 1998), and does not impose any phase shift. The pitch and roll angles are then given by

$$\alpha = \text{tilt}_x \quad \text{and}$$
$$\beta = \sin^{-1}\left[\frac{\sin(\text{tilt}_y)}{\cos(\text{tilt}_x)}\right]. \tag{4}$$

The pitch and roll angles for the two systems were calculated from the entire cruise dataset and the average values were found to be $\alpha = 2.48°$, $\beta = -1.42°$ (Leeds), and $\alpha = -0.01°$, $\beta = -0.11°$ (NOCS), with standard deviations of 0.15°, 0.62°, 0.14°, and 0.64°, respectively. With 1019 fifteen-minute records, these result in standard errors about the mean of approximately 0.01° for the pitch offsets and 0.02° for roll. The measurements from each system can now be rotated into reference frames that share a common $x$–$y$ plane, but which have an unknown yaw offset between them. Note that the mean value of the roll angle over any given data record is highly dependent upon the heeling of the ship due to side winds, sea state, and operations such as deployment of equipment over the side; the mean pitch varies rather less, but does show a positive trend over the duration of the cruise that is assumed to be due to the changing distribution of ballast as fuel is used up. Using different subsets of the data will produce slightly different values of mean pitch and roll angles for each system. We are concerned only with the difference in orientation between the two systems, and provided the measurements from each are obtained over the same time periods, such absolute variations have no impact on the results.

The yaw offset between the two systems is more challenging to determine precisely from the cruise data. An initially attractive approach is to examine the correlation between the accelerations measured by the two systems as a function of applied yaw offset after rotating one set into the coordinate frame of the other on the basis that a maximum correlation should be obtained when the correct yaw is applied. This approach fails—producing inconsistent results across different data records—because the acceleration vectors at the two measurement points differ. The Leeds system is several meters higher than the NOCS system and, thus, experiences a greater acceleration as the ship rolls, the center of roll being close to the waterline. The accelerations due to pitching of the ship are much closer since the relative difference in distance between the two systems and the center of pitch rotation—approxi-

mately amidships, some 40 m aft of the foremast—is much smaller than that for roll. The net result is that the mean difference between the acceleration vectors over a data record depends upon the wave field, and the response of the ship to it.

The approach adopted here is based on a test of the performance of the entire motion correction algorithm via an examination of the frequency-weighted cospectra and ogive functions (Friehe et al. 1991; Brooks and Rogers 2000) for the momentum flux. The rotation rates from the NOCS system are rotated into the Leeds reference frame using a range of assumed yaw offset angles between ±10°—the limiting values being chosen to encompass the possible range of the true offset—and the motion correction algorithm applied. Figure 3a shows example cospectra in which the turbulent wind measurements have been corrected with different assumed yaw offsets. Outside of the frequency range of the wave-induced ship motions the cospectra are almost identical; between about 0.07 and 0.12 Hz, however, there is significant ship motion and the cospectra change substantially with the yaw offset applied. With assumed yaw offsets of ±10° applied, there is substantial spectral energy at wave scales, resulting from a failure of the motion correction algorithm to adequately remove the ship motion from the wind measurements. The absolute magnitude of the peaks within the wave scale decreases as the yaw offset applied approaches the true value and more of the ship motion is removed from the wind measurements. By minimizing the variance of the frequency-weighted cospectra within the frequency range of the ship motion, a value for the yaw offset can be estimated. Since the cospectra are inherently noisy, results from individual records may differ significantly, and substantial averaging may be required. Averaging a total of 28 such estimates, drawn from several days during which significant wave heights ranged from 3 to 5 m, inducing substantial ship motion, an offset of +2.5° ±0.5° is obtained here. Figure 3b shows the corresponding ogive functions for the cospectra in Fig. 3a; these indicate that the error in the final flux estimates associated with yaw offset errors of a few degrees are actually rather small. An assessment of the errors associated with all the angular offsets is given in section 3.

This approach is similar in principle to the commonly adopted approach of maximizing covariance in order to determine a time lag between series, as used above. Some care is required when applying such methods; it would be tempting to think that maximizing the momentum flux as a function of yaw offset in this case might allow the correct offset to be determined. Examination of Fig. 3b, however, shows that the calculated flux increases continuously as the yaw offset is varied from less than the true value to greater.

### c. *Alignment of sonic anemometer and motion pack*

Throughout the discussion above it has been assumed that the measurement axes of the motion pack and sonic anemometer are perfectly aligned; this can be difficult to achieve in practice. An ideal solution is to ensure that the mounting of the anemometer and collocated accelerometers is reproducible in the laboratory, and between installations, and to determine the angular offsets from a laboratory calibration. The Leeds anemometer and motion pack were both mounted on a solid plate in such a manner that they could be accurately repositioned after removal. The pitch and roll offsets were then determined by leveling the mounting plate so that the accelerometers indicated zero tilts, and then taking the indicated anemometer inclinations. This process was repeated, leveling the plate from both positive and negative initial tilt angles to account for any biases, and the results averaged. The yaw offset was then determined by orienting the system such that the $x$ axis of the motion pack was horizontal, and the $y$ axis tilted upward to give a significant roll angle. The tilts reported by the anemometer were used to calculate the $x$, $y$, and $z$ components of the gravitational acceleration along the anemometer measurement axes; these were then rotated into the $x$–$y$ plane of the motion pack using the pitch and roll offset angles. Any difference in the rotated $x$ acceleration ($a'_x$) from zero is a result of the yaw offset, which is then given by

$$\sin\gamma = \frac{a'_x}{g\sin\beta}. \tag{5}$$

The plate was then repositioned with a different roll angle, the process repeated, and the results averaged to obtain a final estimate of the yaw offset. If the pitch and roll offset calibrations are accurate, the calculated yaw offset should be consistent across all roll angles used. The pitch, roll, and yaw offsets of the sonic anemometer axes from our accelerometers were determined to be −1.25° ± 0.04°, −0.06° ± 0.05°, and −6.7° ± 0.2°, respectively. The large yaw offset results from a deliberate rotation of the anemometer so that the mounting bolts were hard against one end of the slots in its base, facilitating precise realignment. A repeated calibration after removal and repositioning of the sonic produced results within 0.1° of the original calibration, giving confidence in the close reproducibility of the alignment between installations. A first step in all subsequent processing of the anemometer data is the rotation of the

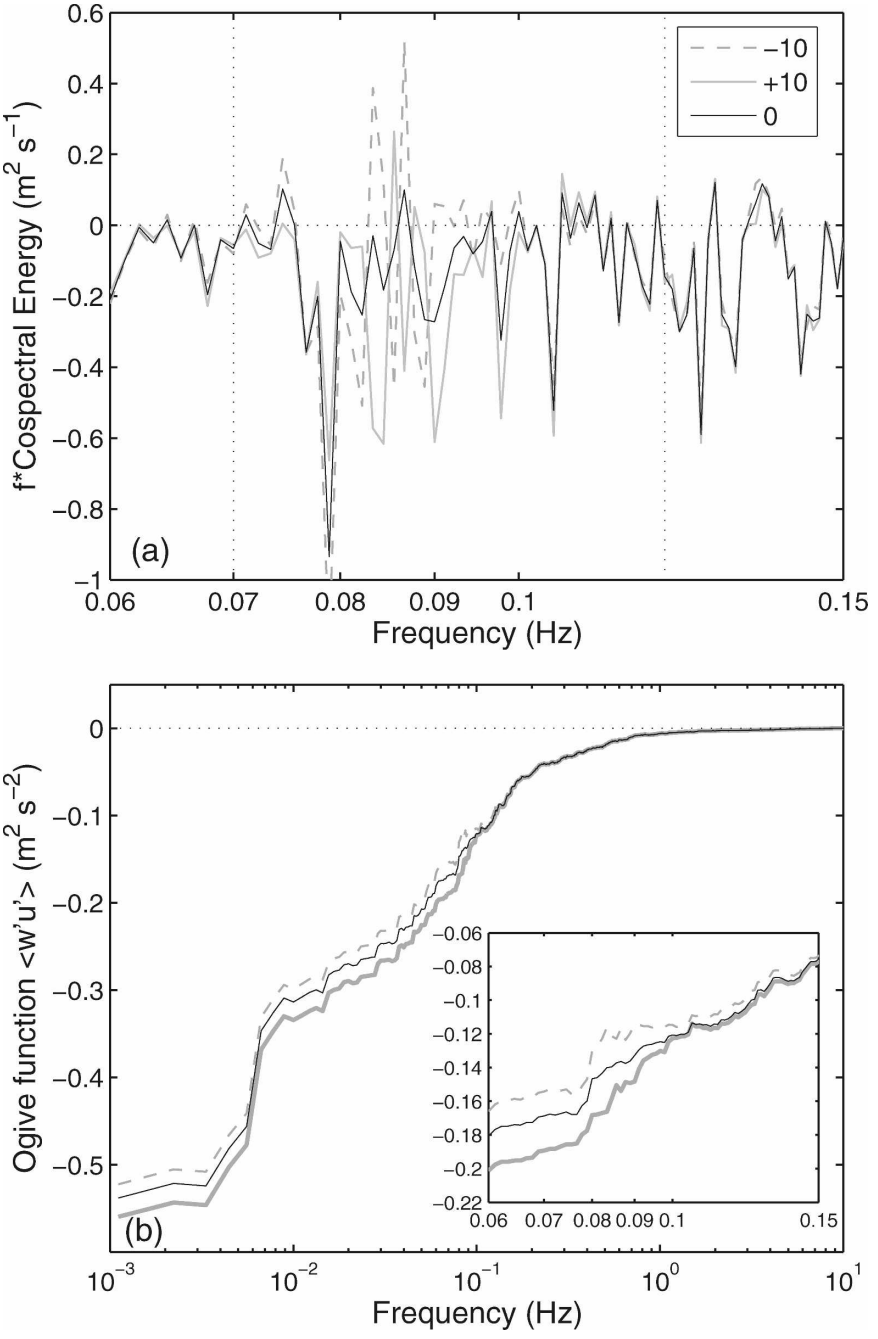


FIG. 3. (a) Frequency-weighted cospectral energy for the momentum flux, with assumed yaw offsets of −10°, 0°, and 10°. Only the narrow range of frequencies associated with the ship motion are shown here; the cospectra are essentially identical outside this range. (b) The corresponding ogive functions showing the full frequency range and (inset) the same range as in (a). Note that the "step" in the ogive curve at around $6 \times 10^{-3}$ Hz is at a much lower frequency than the wave-scale motions, and results from nonstationarity or mesoscale variability in this data record.

measured wind components into the reference frame of the accelerometers.

We can also follow the approach used in section 2b to determine the pitch and roll offsets of the anemometer from the accelerometer axes using the underway inclinometer measurements. This produced mean anemometer pitch and roll angles from the horizontal plane of 1.29° and −0.87°, respectively, with standard deviations

of 0.13° and 0.67°. Using the laboratory-calibrated yaw offset angle of −6.7°, we can determine the net pitch and roll offsets between the anemometer and accelerometer axes: −1.33° and 0.25° (with standard deviations of 0.16° and 0.12°). The pitch offset is in agreement with the laboratory calibration to well within the limits of uncertainty of the measurement; the roll offset differs from the laboratory calibration by about 0.3°, just over twice the uncertainty in the measurements. This difference is likely due to the reproducibility of the alignment between installations being slightly underestimated in the repeated laboratory calibration.

The methodology used to determine the yaw offset between the Leeds and NOCS motion packs can also be applied to the anemometer. Using the entire cruise dataset, and a range of yaw offset angles from −17° to 6° (±10° about the laboratory-calibrated value), the full motion correction algorithm was run, and the yaw offsets producing minima in the variance of the frequency-weighted cospectra for the along-wind stress determined. The scatter in individual values is large, spanning the full range of yaw offsets applied; the mean value, however, was −7.2° with a standard deviation of 5.0° and a standard error of ±0.3°. The difference from the laboratory calibration is equal to the sum of their respective error estimates. It should be noted that in this case the yaw offset between the anemometer and motion pack does not affect all of the velocity components: Assuming the pitch and roll offsets are accurately corrected, then the vertical velocity component and the motion pack $z$ axis are aligned, and the vertical velocity is properly corrected, while the horizontal velocity components are not.

If both sets of yaw offsets are unknown, then the problem is probably intractable. One could attempt to apply the methodology while varying both anemometer–accelerometer and rate-gyro–accelerometer yaw offset angles, finding the minimum in the 2D field of mean stresses. This represents a considerable processing task and no attempt has been made to test it here.

An implicit assumption in this process is that the anemometer inclinometers are aligned with the wind measurement axes. The resolution of the inclinometers in the Gill anemometer is 0.01°, but the stated absolute accuracy is much lower at 0.3° with a null repeatability of 0.15°. The laboratory calibration discussed above achieved a rather better repeatability, with a range of 0.05°, the resolution of angular measurements (near the horizontal) based on the accelerometers. The manufacturer's quoted accuracy refers to the precision with which the inclinometers are aligned with the wind measurement axes, which is more difficult to assess. The limiting factor in aligning the anemometer measurements with those of the motion pack is thus the manufacturer's calibration of the internal alignment.

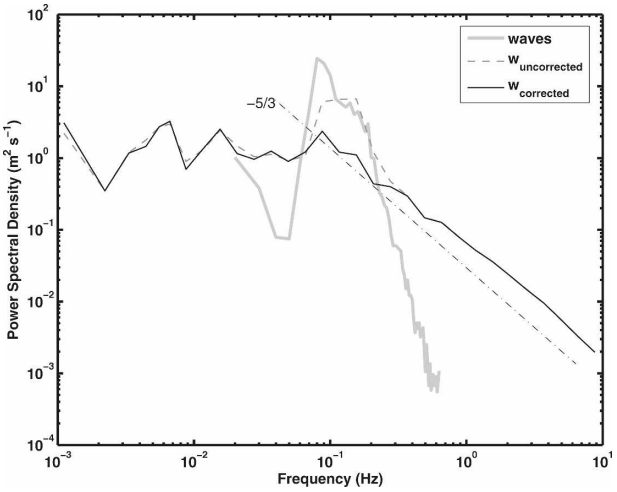


FIG. 4. Power spectral density of the uncorrected (gray dashed) and corrected (black solid) vertical wind components, along with that of the waves (pale gray, solid). A −5/3 slope is shown for reference.

## 3. Error analysis

### a. Motion correction

To demonstrate the effective application of the approach discussed above, some example data from the SEASAW cruise D317 are presented. Figure 4 shows the power spectral density of the vertical wind component before and after motion correction, along with that of the ocean waves derived from the shipborne wave recorder (Tucker and Pitt 2001) for a 15-min data record on 25 March 2007, with a significant wave height of approximately 4 m. The wave-scale contributions to the vertical wind are effectively removed. The frequency-weighted cospectral density and ogive functions for the kinematic wind stress are shown in Fig. 5, both before and after motion correction. There is no indication of wave-scale contamination of the momentum flux after motion correction. The ogive function converges by a frequency of about 0.003 Hz (a period of approximately 5.5 min) indicating that a 15-min averaging time is ample to include all scales contributing to the flux—a typical value for near-surface measurements. Figure 6 shows a comparison of the along-wind momentum flux determined via eddy correlation with that determined from the inertial dissipation technique (Large and Pond 1981; Yelland et al. 1994) for both the motion-corrected and uncorrected wind measurements. Also shown are the eddy correlation estimates plotted

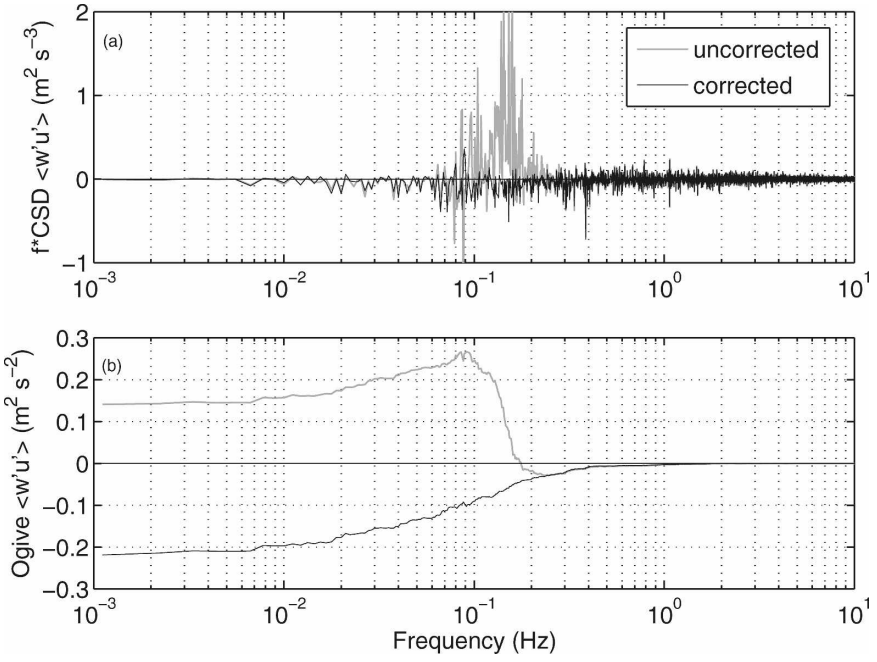


FIG. 5. (a) Frequency-weighted cospectral density and (b) ogive function for the along-stream kinematic wind stress, $\overline{w'u'}$ (m$^2$ s$^{-2}$) for the same period as in Fig. 5. The gray lines show the results for prior to motion correction; black lines show the after motion correction.

against those from the NOCS system for the same time periods. Data from the entire cruise are included, but are restricted to records for which the mean wind direction is within 30° of the bow and the ship is hove to; no further quality control has been applied at this stage. The motion-corrected estimates lie around the one-to-one line for both the inertial dissipation estimates and the NOCS data, with scatter typical of such measurements (see, e.g., Anctil et al. 1994). The Leeds estimates are biased slightly low compared to the NOCS estimates, and there are a dozen or so points where the Leeds estimates are biased very high compared to both the inertial dissipation and the NOCS values. These are associated with records that suffer large contributions to the flux at frequencies an order of magnitude or more lower than that of the wave motion; this is indicative of nonstationarity in the turbulence, or maneuvering of the ship. Exact agreement between the two eddy covariance systems cannot be expected since the NOCS system is situated approximately 3 m lower than the Leeds system and, thus, experiences a slightly lower mean wind speed; the effects of flow distortion will also be different at the two sites (Yelland et al. 1998, 2002) introducing further discrepancies. The uncorrected eddy covariance results are all strongly biased, and mostly represent physically unrealistic positive (upward) fluxes of momentum. The uncorrected fluxes show a far larger difference from the corrected values than those reported by Schulze et al. (2005), obtained under much lower significant wave heights, emphasizing the strong effect of wave motions on the measurements.

Although the inertial dissipation technique is not affected by low-frequency platform motion, and is much

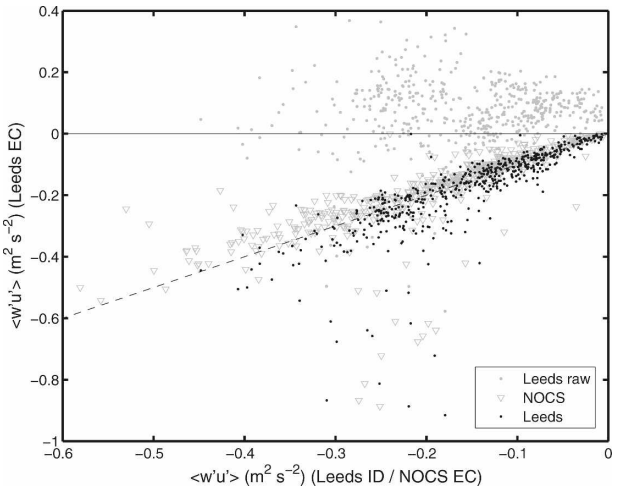


FIG. 6. Comparison of 15-min-average values of the along-wind momentum flux calculated via eddy correlation and inertial dissipation techniques for the uncorrected (gray dots) and motion-corrected (black dots) Leeds measurements. For comparison, the motion-corrected fluxes are also shown plotted against the motion-corrected NOCS EC fluxes (▽).

TABLE 1. The RMS errors, mean biases, and maximum error on individual records (percentages) resulting from +1° offsets between pitch, roll, or yaw measurement axes for the motion sensors (accelerometer–rate-gyro) and anemometer–accelerometers. The primary values are derived from records where the magnitude of the momentum flux was greater than 0.01 $m^2 s^{-2}$; those in brackets are derived from the entire dataset.

| | Pitch | Roll | Yaw |
|---|---|---|---|
| Motion sensor | | | |
| RMS error | 0.14% (0.2%) | 0.26% (0.3%) | 0.74% (0.8%) |
| Mean bias | 0.001% (0.01%) | −0.02% (−0.02%) | 0.38% (0.37%) |
| Max error | 0.9% (1%) | 1.8% (2%) | 3% (3%) |
| Motion anemometer | | | |
| RMS error | 3.2% (29%) | 3.7% (16%) | 0.7% (14%) |
| Mean bias | 1.8% (3.1%) | 0.8% (2%) | 0.3% (0.9%) |
| Max error | 19% (650%) | 32% (330%) | 5.5% (310%) |

less sensitive to flow distortion than eddy covariance (Fairall et al. 1990), it relies upon assumptions of local isotropy and the validity of Monin–Obukhov similarity and there remain questions as to its applicability over ocean waves. It is, however, widely used and there is substantial evidence that it is applicable under most conditions (Fairall et al. 1990; Taylor and Yelland 2001). Here, the good general agreement between the inertial dissipation and the eddy covariance momentum fluxes, and between the eddy covariance estimates from the two separate systems, suggests that the motion corrections of both the Leeds and NOCS systems have been effective. This is supported by the examination of individual spectra and cospectra such as those in Figs. 4 and 5.

### b. Position offset errors

The position vector offset between the accelerometers and the location of the wind measurements results in a linear velocity at the measurement point due to rotation about the accelerometers. This must be determined with a degree of accuracy sufficient to limit the uncertainty in the rotational velocity to an acceptable level—ideally to less than the resolution of the sonic anemometer. The linear velocity due to rotation about any given axis is $rd\theta/dt$, where $\theta$ is in radians and $r$ is the position offset between sensors; the maximum rotation rate observed here was a roll of almost 8° $s^{-1}$ (0.135 rad $s^{-1}$) with significant wave heights of approximately 5 m; rounding this up to 10° $s^{-1}$ (0.174 rad $s^{-1}$) and taking the sonic anemometer resolution of 0.01 m $s^{-1}$, we get a required position offset accuracy of 0.057 m. This is readily achievable for small separations—an accuracy an order of magnitude better than this was achieved for the Leeds system with a position offset of $\Delta x = 0.81$ m, $\Delta y = 0.18$ m, $\Delta z = 0.67$ m (all $\pm$ 0.005 m)—but becomes increasingly difficult to achieve as the sensor separation increases and direct measurement becomes impractical.

### c. Accelerometer–gyro alignment errors

Alignment errors between the accelerometer and rate-gyro measurement axes impact upon the motion correction in two ways: through accumulated errors in the derived platform velocity components in the earth frame, and through errors in the additional velocity component at the anemometer head due to rotation about the accelerometers. The latter also depends upon the position offset between the accelerometers and the anemometer. For the installation considered here, the maximum rotationally induced velocity was approximately 0.08 m $s^{-1}$ for rolling of the ship. For uncertainties of less than about 10°, the fractional error in this velocity resulting from a misalignment is less than the anemometer resolution and can be neglected. The errors in the platform velocity are more significant. To assess their impact on the momentum flux, the complete motion correction algorithm was run with deliberate offsets of +1° in pitch, roll, and yaw in turn, and the calculated momentum flux compared with that with no additional angular offsets. The RMS and maximum fractional errors and mean biases are given in Table 1. There is considerable scatter with errors in individual estimates of up to 3%; however, the maximum mean bias is just under 0.4%. The uncertainty in our estimates of the angular alignment of the spatially separated motion sensors is much smaller than this and, thus, does not impact significantly upon the mean stress estimates.

### d. Anemometer alignment errors

Any error in the alignment of the anemometer and motion pack measurement axes will result in biasing of the calculated momentum flux. To assess the severity of this bias, the momentum flux was calculated with separate pitch, roll, or yaw offsets of 1° applied to the wind components before carrying out the motion correction. The RMS and maximum errors, as well as the mean

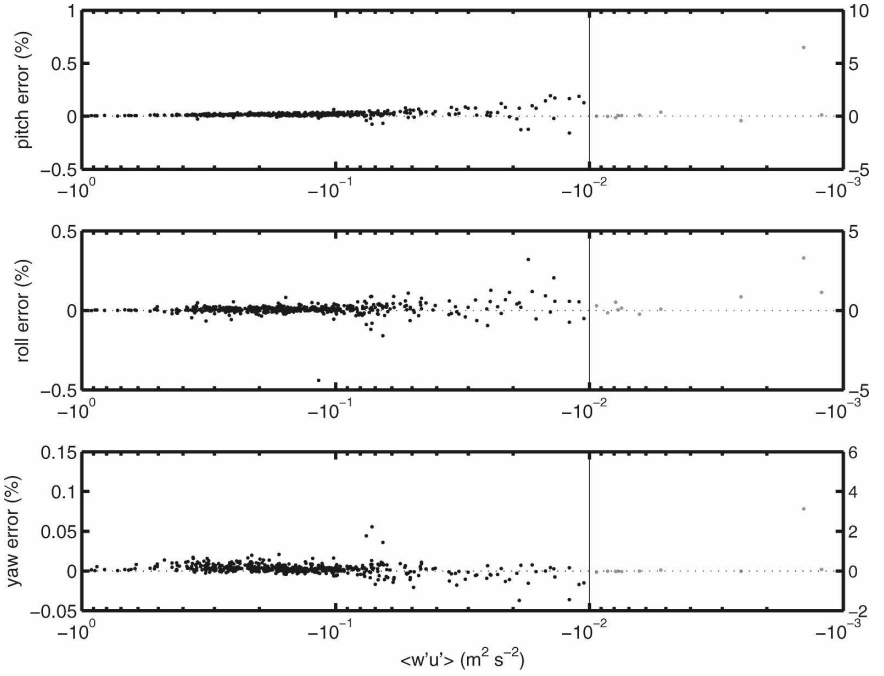


FIG. 7. The errors in wind stress (%) resulting from 1° offsets in pitch, roll, and yaw between the sonic anemometer and motion pack axes plotted against the mean stress. Note that the vertical scales change by factors of 10 (pitch, roll) and 40 (yaw) at a mean stress of −0.01 $m^2 s^{-2}$ indicated by the vertical lines.

bias over the whole dataset, are given in Table 1. The errors are much larger than for the misalignment of the motion sensors, with a maximum bias of 3.1% and an RMS error of 29% for an error in the pitch offset. The errors in some individual estimates are very large—up to a factor of 6.5; however, these large fractional errors typically result from low absolute values of the stress. Figure 7 shows the errors plotted against the stress. If we exclude the small number of records where the magnitude of the stress is less than 0.01 $m^2 s^{-2}$, then more representative estimates of the errors are obtained. The maximum mean bias is now 1.8% (for pitch) and the maximum RMS error is 3.7% (for roll).

Figure 8 shows an example of the impact on a single data record for a much wider range of angular offsets. The biases typically change sign with the sign of the angular offset, and increase in magnitude with the offset angle; the dependence is approximately linear for small angles, but note that the roll and yaw biases here exhibit a maximum (minimum) at around +3.5° (−3.5°) for the along-wind (crosswind) momentum flux. Figure 9 shows ogive curves for the along-wind momentum flux with pitch offsets of 0°, ±1°, and ±5°. The curves diverge only slightly at high frequencies, but to a much greater extent within the frequency range of the ship motion. The bias in individual flux estimates due to axis misalignment will thus be dependent upon the wave state and the ship's motion. This implies that the relative importance of pitch, roll, and yaw offsets on the momentum flux components is also likely to change with changing platform motion.

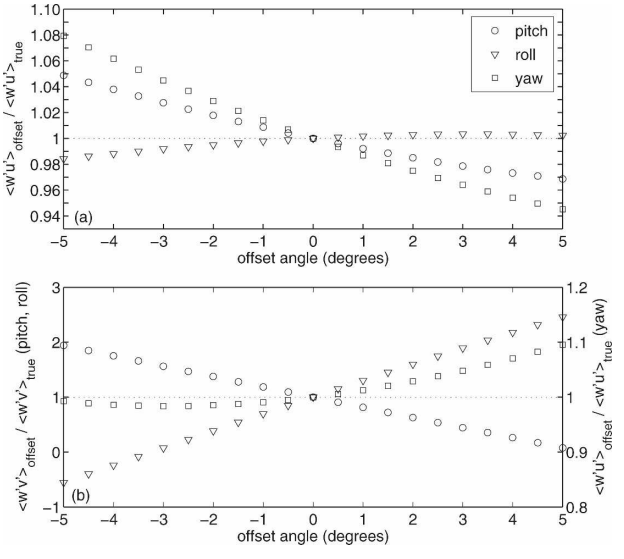


FIG. 8. An example of the ratios of the biased flux estimates to the best estimate for (a) along-wind and (b) crosswind momentum flux components as a function of pitch, roll, and heading offsets between the anemometer and motion pack measurement axes [note change of *y* scale for yaw in (b)].

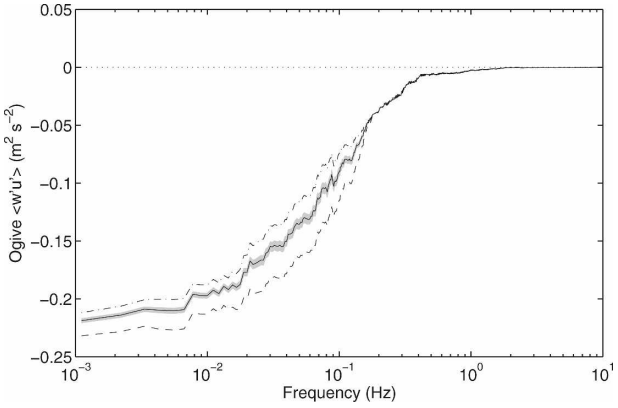


FIG. 9. Ogive curves for the along-wind momentum flux for accurate alignment of the anemometer and motion-sensing axes (solid line), and pitch offsets of ±1° (gray area), +5° (dotted–dashed line), and −5° (dashed line).

Figure 10 shows the fractional and absolute errors in the stress resulting from 1° offsets between the anemometer and accelerometer axes as functions of the significant wave height. In all cases the absolute errors increase in magnitude with wave height; the fractional error also increases with wave height for yaw offsets, while the pitch and roll offsets show no distinct trend. Excluding the extreme errors at very low mean stress values, the yaw offset results in the smallest individual errors and mean bias; the roll offset produces the largest individual errors; the pitch offset results in smaller individual errors than those for roll, but a strongly skewed distribution results in the largest mean bias. These errors are similar to those reported by Schulze et al. (2005) for their determination of motion correction using multiple sets of paired accelerometers; note, however, that the uncertainties in the offset angles here are mostly much smaller than the 1° perturbations used in the error analysis, and the significant wave heights encountered here are a factor of 5 larger than those experience by Schulze et al. The mean biases in the wind stress associated with our estimated errors in pitch, roll, and yaw alignment are approximately 0.1%, 0.1%, and 0.2%. Those associated with the 0.3° uncertainty in alignment of the sonic anemometer's internal inclinometer are 0.5% for pitch and 0.24% for roll. Both here, and in the Schulze et al. study, the estimated biases are smaller than the statistical uncertainty of the stress estimates.

## 4. Conclusions

A method has been demonstrated for correlating the data from independently logged and spatially separated motion packs, and for determining the angular offsets between the measurement axes of the two systems. The combined data have been used to correct sonic anemometer measurements of the turbulent wind for platform motion following Edson et al. (1998), and the effective removal of wave-scale motion from the turbulence spectra demonstrated. Estimates of wind stress calculated via eddy correlation from the motion-corrected data are shown to be in general agreement with those determined both via the inertial dissipation technique and via eddy correlation from an independent system.

Although the combination of measurements from separate motion sensing systems was forced here by the

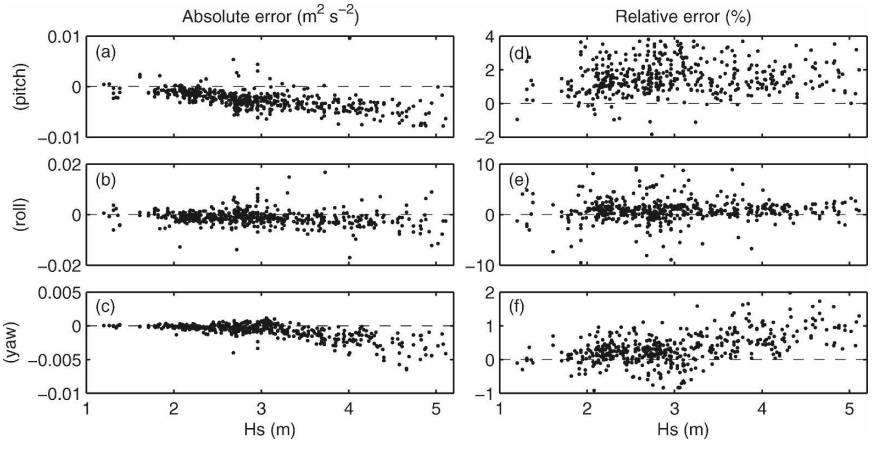


FIG. 10. (left) Fractional and (right) absolute errors in the wind stress resulting from a 1° offset in pitch, roll, or yaw between the anemometer and motion pack measurement axes. The fractional error figures have been cropped to omit a small number of outliers for the sake of clarity.

partial failure of one system, the methods outlined can be applied more generally in order to allow the utilization of a single high-specification (and expensive) motion pack along with relatively inexpensive sets of three-axis accelerometers collocated with sonic anemometers to improve the fidelity of motion correction from multiple measurement sites on a single moving platform.

Estimates of the biases in the components of the momentum flux due to the misalignment of anemometer and motion pack axes have been made. These are shown to be dependent on the motion of the platform and, hence, sea state. The errors arising from misalignment of the rate gyro and accelerometer axes are relatively small, with the yaw offset being most important; an offset of 1° contributes to a mean bias of ~0.4%. The errors arising from misalignment of the measurement axes of the anemometer and motion sensors are much more significant, with the pitch offset contributing the largest mean bias, 1.8% for a 1° offset, and the roll offset the largest contribution to the RMS error 3.7% for a 1° offset. A 1° yaw offset contributes a negligible 0.3% bias. Accurate alignment of the anemometer and motion pack requires either reproducibility of a careful laboratory alignment, or the availability of internal inclinometers; these are available on very few models of sonic anemometer, but greatly ease the accurate determination of alignment.

Given the rotation rates experienced during the cruise, the position offset between the anemometer measurement volume and the accelerometers must be determined to a precision of better than about 0.06 m in order to reduce the resulting uncertainty in the rotationally induced velocity of the measurement volume to less than the resolution of the anemometer; this is readily achieved for collocated sensors and is exceeded by an order of magnitude here.

Some of the scatter between the Leeds and NOCS results presented here, and in particular some of the larger discrepancies, may result from differences in flow distortion at the different measurement sites. The impact of the mean flow distortion on inertial dissipation estimates of the wind stress has been studied by Yelland et al. (1998, 2002), and the relevant corrections applied here. The impact on eddy covariance estimates of the wind stress of time-varying flow distortion, as a function of ship attitude and motion, is entirely unknown; addressing this question is beyond the scope of this paper but will be the subject of future investigation.

*Acknowledgments.* SEASAW is a U.K.-SOLAS project, funded by the Natural Environment Research Council under Grant NE/C001842/1. Thanks to Margaret Yelland and Robin Pascal for provision of the NOCS data and comments on an early draft of the paper.

## REFERENCES

Anctil, F., M. A. Donelan, W. M. Drennan, and H. C. Graber, 1994: Eddy-correlation measurements of air–sea fluxes from a discus buoy. *J. Atmos. Oceanic Technol.,* **11,** 1144–1150.

Brooks, I. M., and D. P. Rogers, 2000: Aircraft observations of the mean and turbulent structure of a shallow boundary layer over the Persian Gulf. *Bound.-Layer Meteor.,* **95,** 189–210.

——, and Coauthors, 2007: An overview of the Sea Spray, Gas Flux, and Whitecaps (SEASAW) field study. Preprints, *15th Conf. on Air–Sea Interaction,* Portland, OR, Amer. Meteor. Soc., P1.3. [Available online at http://ams.confex.com/ams/pdfpapers/124982.pdf.]

Edson, J. B., A. A. Hinton, K. E. Prada, J. E. Hare, and C. W. Fairall, 1998: Direct covariance flux estimates from mobile platforms at sea. *J. Atmos. Oceanic Technol.,* **15,** 547–562.

Fairall, C. W., J. B. Edson, S. E. Larsen, and P. G. Mestayer, 1990: Inertial-dissipation air–sea flux measurements: A prototype system using real-time spectral computations. *J. Atmos. Oceanic Technol.,* **7,** 425–453.

Friehe, C. A., and Coauthors, 1991: Air–sea fluxes and surface layer temperatures around a sea-surface temperature front. *J. Geophys. Res.,* **96,** 8593–8609.

Graber, H. C., E. A. Terray, M. A. Donelan, W. M. Drennan, J. Van Leer, and D. B. Peters, 2000: ASIS—A new air–sea interaction spar buoy: Design and performance at sea. *J. Atmos. Oceanic Technol.,* **17,** 708–720.

Large, W. G., and S. Pond, 1981: Open ocean momentum flux measurements in moderate to strong winds. *J. Phys. Oceanogr.,* **11,** 324–336.

Lenschow, D. H., 1986: Aircraft measurements in the atmospheric boundary layer. *Probing the Atmospheric Boundary Layer,* D. H. Lenschow, Ed., Amer. Meteor. Soc., 39–55.

——, and P. Spyers-Duran, 1989: Measurement techniques: Air-motion sensing. RAF Research Bull. 23, NCAR, 36 pp.

Schulze, E. W., B. G. Sanderson, and E. F. Bradley, 2005: Motion correction for shipborne turbulence sensors. *J. Atmos. Oceanic Technol.,* **22,** 44–69.

Taylor, P. K., and M. J. Yelland, 2001: Comments on "On the effect of ocean waves on the kinetic energy balance and consequences for the inertial dissipation technique." *J. Phys. Oceanogr.,* **31,** 2532–2536.

Tucker, M. J., and E. G. Pitt, 2001: *Waves in Ocean Engineering*. Ocean Engineering Book Series, Vol. 5, Elsevier, 521 pp.

Yelland, M. J., P. K. Taylor, I. E. Consterdine, and M. H. Smith, 1994: The use of the inertial dissipation technique for shipboard wind stress determination. *J. Atmos. Oceanic Technol.,* **11,** 1093–1108.

——, B. I. Moat, P. K. Taylor, R. W. Pascal, J. Hutchings, and V. C. Cornell, 1998: Wind stress measurements from the open ocean corrected for air flow distortion by the ship. *J. Phys. Oceanogr.,* **28,** 1511–1526.

——, ——, R. W. Pascal, and D. I. Berry, 2002: CFD model estimates of the airflow distortion over research ships and the impact on momentum flux measurements. *J. Atmos. Oceanic Technol.,* **19,** 1477–1499.